New Models and Numerical Codes for Shockwave Processes in Condensed Media

Proceedings

Editor Dr I.G. Cameron

St Catherines College, Oxford
15-19 September, 1997

International Workshop

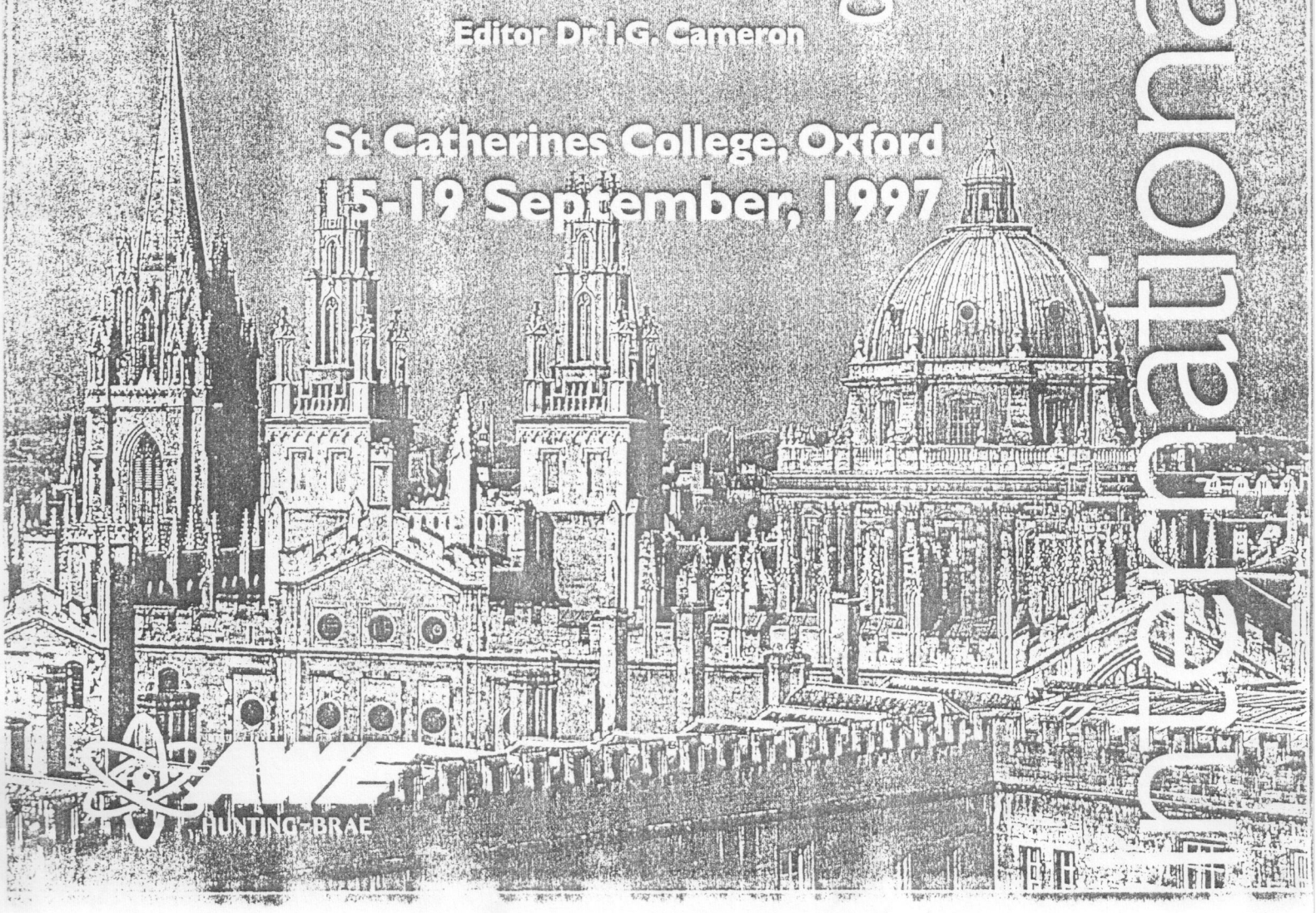

HUNTING-BRAE

International Workshop

Published by AWE Hunting - BRAE
Director Physics Research

Aldermaston, Reading, Berkshire RG7 4PR

Series ISBN 0 9532966 0 1
Vol.1 ISBN 0 953 2966 1 X
Vol.2 ISBN 0 952 2966 2-8

CALCULATIONAL TECHNIQUE FOR SHOCK WAVES WITH ELEVATED MONOTONOCITY

V.F.Kuropatenko, I.R.Makeeva

Russian Federal Nuclear Center - VNIITF
P.O.Box 245, 456770 Snezhinsk, Chelyabinsk region, Russia

1. INTRODUCTION

Many techniques for the calculation of both continuous and discontinuous solutions of continuous mechanics are known. All of them possess different dispersing and oscillation properties. For example, Neumann-Richtmayer technique [1] where specially introduced pseudoviscosity is used for calculation of energy dissipation on shock wave front give the solution with oscillations both behind the shock front and on rarefaction wave. Oscillation amplitude damps with time. Godunov technique [2] where relations for arbitrary discontinuity decay are used to determine auxiliary parameters on calculational mesh bounds is monotonic but possesses strong dispersing properties. The higher nonmonotonicity or dispersion of difference technique the greater error have this technique in determination of fractures and phase transformation origins.While calculating shock and rarefaction wave interaction with each other or with contact bounds irreversible accumulation of errors outcoming from oscillation and dispersing properties of difference technique. This fact enlarges difference between characteristics of real physical processes and its mathematical interpretation.

Thus one of important ways of error reduction of numerical solution for problems with interacting discontinuities is minimization of difference technique dispersion and oscillation. Difference technique for calculation of continuous media mechanics equations so called "KAMA-97" is considered below. In this technique minimization of oscillation and dispersing properties is achieved by choice of specific form of difference equations and application of Hugoniot-Renkin relations for energy dissipation description inside of shock layer which replace strong discontinuity for difference calculation.

To verificate the technique a set of standard tests such as stationary shock wave, rarefaction wave was calculated. The same tests were calculated using other techniques such as Neumann-Richtmayer, Lax-Wendroff ones, technique earlier proposed by one of the authors of [4], Godunov technique [2]. Numerical results are shown on plots.

2. METHOD

Let the matter motion and variation of thermodynamic parameters is described by the system of differential equations of ideal continuous media with respect to Lagrangian coordinates:

$$\frac{\partial V}{\partial t} - \frac{\partial u}{\partial m} = 0, \tag{1}$$

$$\frac{\partial u}{\partial t} + \frac{\partial P}{\partial m} = 0, \tag{2}$$

$$\frac{\partial E}{\partial t} + P\frac{\partial V}{\partial t} = 0, \tag{3}$$

$$P = f(V,E), \tag{4}$$

$$\frac{\partial x}{\partial t} = U \tag{5}$$

where V is specific volume, U is mass velocity, P is pressure, E is specific internal energy, t is time, m is mass Lagrangian coordinate, x is Euleran coordinate.

On the shock front the conservative laws are represented in form of Hugoniot-Renkin relations:

$$(V_+ - V_-)W + (u_+ - u_-) = 0, \tag{6}$$

$$(u_+ - u_-)W - (P_+ - P_-) = 0, \tag{7}$$

$$E_+ - E_- + 0.5(P_+ + P_-)(V_+ - V_-) = 0, \tag{8}$$

here quantities with "–" characterize the matter state before the front of discontinuity, and with "+" – behind the front.

Let divide an integration region of equation system (1-5) to meshes with mass $h_{i+0.5}=x_{i+1}-x_i$. Let define P, V, Å, U at the center of mesh (in the points with half subscripts), and coordinate x - at the grid nodes (in the points with integer subscripts). At the points with integer subscripts let introduce auxiliary values of velocity and pressure $\overline{U}_i$, $\overline{P}_i$.

Let approximate equations (1,2,5) by difference equations

$$\frac{V_{i+0.5}^{n+1}-V_{i+0.5}^{n}}{\tau}=\frac{\bar{u}_{i+1}^{n+1}-\bar{u}_{i}^{n+1}}{h}, \tag{9}$$

$$\frac{V_{i+0.5}^{n+1}-V_{i+0.5}^{n}}{\tau}=\frac{\bar{u}_{i+1}^{n+1}-\bar{u}_{i}^{n+1}}{h}, \tag{10}$$

$$x_i^{n+1}=x_i^n+\tau\cdot\overline{U}_i . \tag{11}$$

To find auxiliary values $\overline{U}_i$, $\overline{P}_i$ let consider auxiliary meshes of difference grid $\left(x_{i-0.5}^n, x_{i+0.5}^n\right)$. Let divide them to two types. The meshes of the first type are characterized by the condition $U_{i+0.5}^n-U_{i-0.5}^n<0$ (compression) and the meshes of the second type are characterized by the condition $U_{i+0.5}^n-U_{i-0.5}^n\geq 0$ (rarefaction). Auxiliary values $\overline{U}_i$, $\overline{P}_i$ are determined as follows. For the meshes of the first type:

$U_+=U_{i-0.5}^n$, $U_-=U_{i+0.5}^n$, $P_-=P_{i+0.5}^n$, $V_-=V_{i+0.5}^n$, $E_-=E_{i+0.5}^n$, if $P_{i-0.5}^n>P_{i+0.5}^n$,

$U_+=U_{i+0.5}^n$, $U_-=U_{i-0.5}^n$, $P_-=P_{i-0.5}^n$, $V_-=V_{i-0.5}^n$, $E_-=E_{i-0.5}^n$, if $P_{i-0.5}^n\leq P_{i+0.5}^n$. (12)

Values P+, V+, E+, W are found solving the system of equations (4),(6-8). Values U+, P+, are taken as auxiliary values

$$\overline{U}_i=U_+,\ \overline{P}_i=P_+ . \tag{13}$$

For the meshes of the second type auxiliary values of velocity and pressure are found from the system of difference equations

$$\overline{U}_i=\frac{U_{i+0.5}^n+U_{i-0.5}^n}{2}-\frac{\tau}{2h}\left(P_{i+0.5}^n-P_{i-0.5}^n\right), \tag{14}$$

$$\overline{P}_i=\frac{P_{i+0.5}^n+P_{i-0.5}^n}{2}-\frac{\tau\left(\left(a_{i+0.5}^n\right)^2+\left(a_{i-0.5}^n\right)^2\right)}{4h}\left(U_{i+0.5}^n-U_{i-0.5}^n\right) . \tag{15}$$

$$a^2=-\left(\frac{\partial P}{\partial V}\right)_S$$

Here à is mass sound velocity defined by equation

Values $V_{i+0.5}^{n+1}$, $U_{i+0.5}^{n+1}$ in the centers of meshes and a value x_i^{n+1} on the bounds of meshes are found using equations (9-11). To find $E_{i+0.5}^{n+1}$ let divide all basic meshes of difference grid into two types. Again the meshes of the first type are characterized by condition $\overline{U}_{i+1}-\overline{U}_i<0$ and the meshes of the second type are characterized by condition $\overline{U}_{i+1}-\overline{U}_i\geq 0$. For the meshes of the first type let approximate the equation (3) by the following difference equation:

$$\frac{E_{i+0.5}^{n+1}-E_{i+0.5}^{n}}{\tau}=-\frac{1}{2}\left(\overline{P}_{i+0.5}^n+\overline{P}_{i+0.5}^{n+1}\right)\frac{V_{i+0.5}^{n+1}-V_{i+0.5}^{n}}{\tau} \tag{16}$$

Auxiliary value $\overline{P}_{i+0.5}^{n+1}$ is determined solving the system of equations (4),(6-8) where we set:

$$P_-=P_{i+0.5}^n,\ V_-=V_{i+0.5}^n,\ E_-=E_{i+0.5}^n,\ \left|U_+-U_-\right|=\left|\overline{U}_{i+1}-\overline{U}_i\right| \tag{17}$$

For the meshes of the second type new value of energy $E_{i+0.5}^{n+1}$ is determined solving the equation for isentrope $dE+PdV=0$

Then new value of pressure is found using equation of state (4).

To verificate proposed difference technique and compare it with other techniques the following test problems were calculated.

Test 1. Ideal gas with the equation of state

$$P = (\gamma - 1)\,\rho\, E$$

and the following initial parameters:

$$\gamma = 4/3\ ,\ \rho_0 = 1\ ,\quad E_0 = 0\ ,\ P_0 = 0\ ,\ U_0 = 0$$

is situated in a region with coordinates [0.,14.]. Constant velocity U= 3 is set at the left boundary of the system.

According to analytical solution [5] the following parameters are obtained behind the shock front:

$$\rho_1 = 7\ ,\quad E_1 = 4.5\ ,\ P_1 = 10.5\ ,\ U_1 = 3\ ,$$

and the velocity of shock propagation is W=3.5 .

The profiles of pressure and velocity obtained in numerical solution compared with analytical solution and the calculation using technique proposed in [4] are shown in the figures 1,2. One can see a good agreement between numerical and analytical solution but there are practically no differences between two calculations if we deal with such scale.

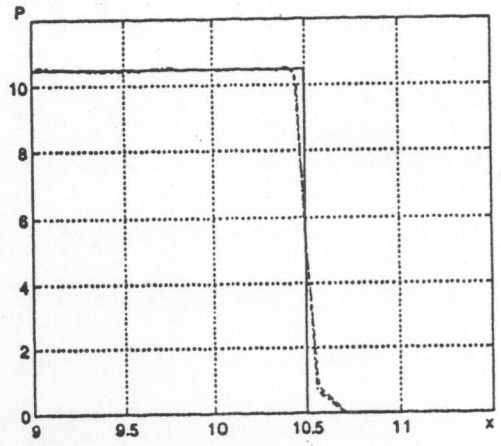

Fig 1 Test1 P versus x co-ordinate

versus

x for the shock wave, t=3.

—— - analytical solution,

— — — - KAMA - 97,

— - — - Technique [4].

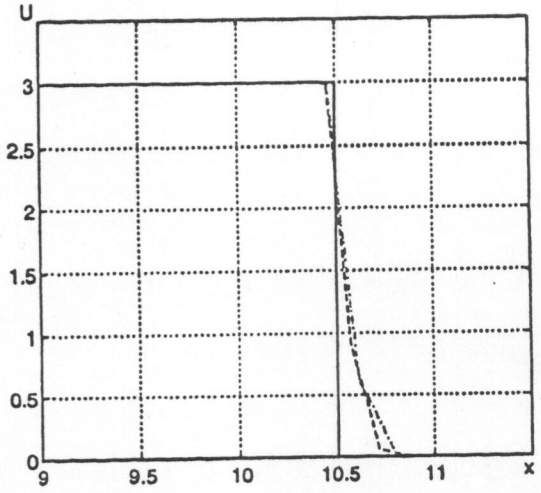

Fig.2. Test 11. The dependence of velocity U

dependence of velocity U versus

coordinate x for the shock wave, t=3.

—— - analytical solution,

— —ú— - KAMA - 97,

—ú—ú— - Technique [4].

To analyze differences between numerical techniques fragments of solution in small vicinity of shock front are shown in figures 3-8. Here proposed technique is compared with techniques described in [1], [3], [4]. One can see that new technique have significantly smaller oscillations behind the shock front.

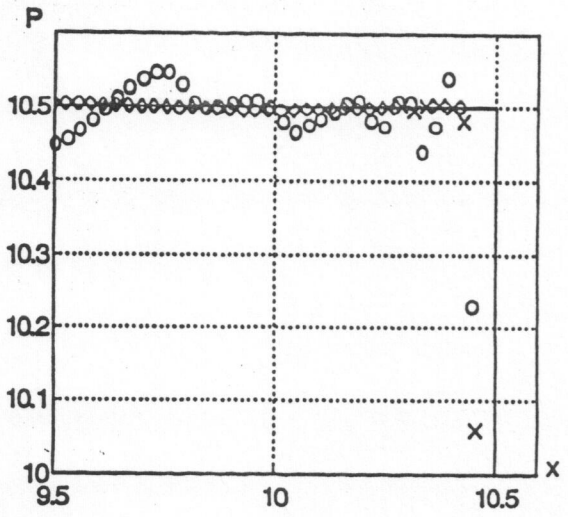

Fig.3. Test ¹1. The dependence of pressure P versus versus
coordinate x for the shock wave. Fragment of the solution.

—— - analytical solution,
x x x - KAMA - 97,
î î î - Technique [4].

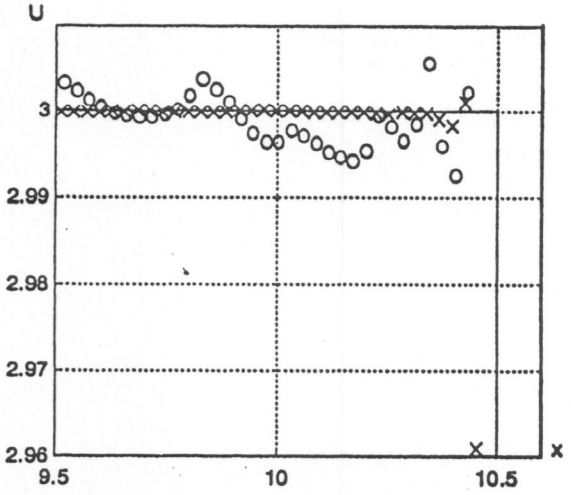

Fig.4. Test ¹1. The dependence of velocity U

coordinate x for the shock wave. Fragment of the solution

—— - analytical solution,
x x x - KAMA - 97
î î î - Technique [4].

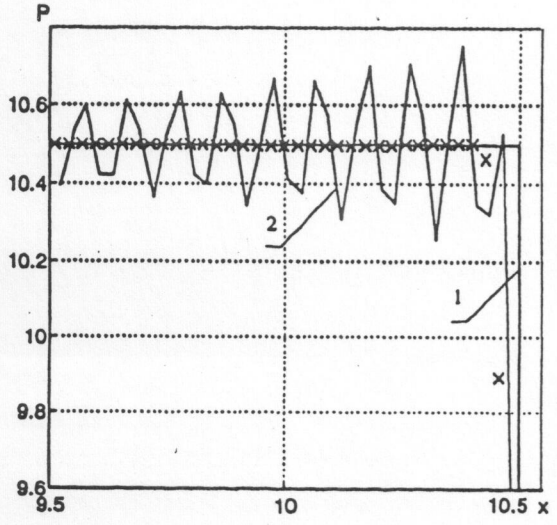

Fig.5. Test ¹1. The dependence of pressure P versus versus
coordinatex for the shock wave. Fragment of the solution

1 - analytical solution,
2 - technique [1],
x x x - KAMA - 97

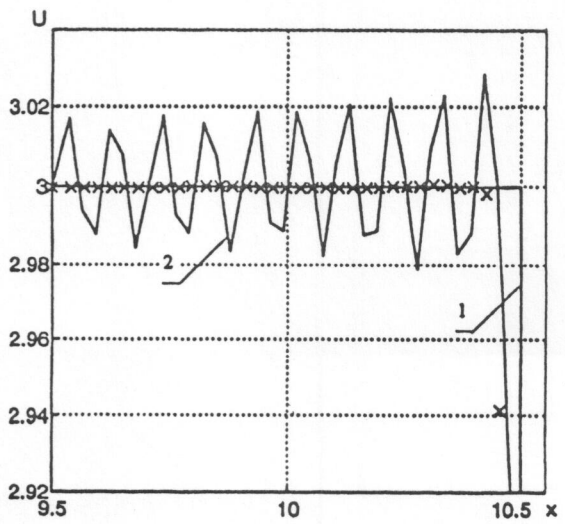

Fig.6. Test ¹1. The dependence of velocity U

coordinate x for the shock wave. Fragment of the solution

1- analytical solution
2 - technique [1],
x x x - KAMA - 97.

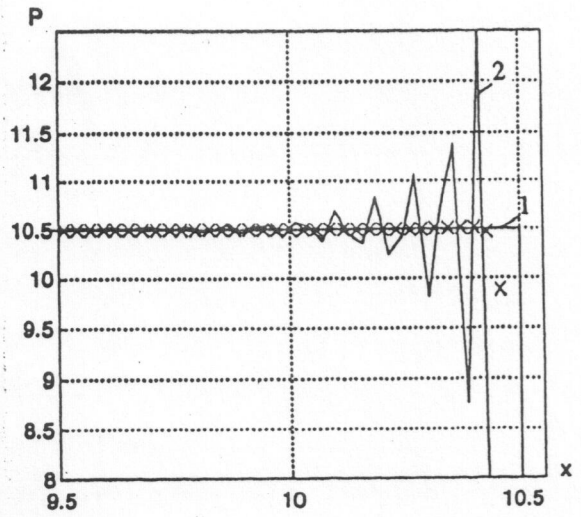

Fig.7. Test ¹1. The dependence of pressure P versus versus coordinate x for the shock wave. Fragment of the solution.
1 - analytical solution,
2 - technique [3],
3 - KAMA - 97.

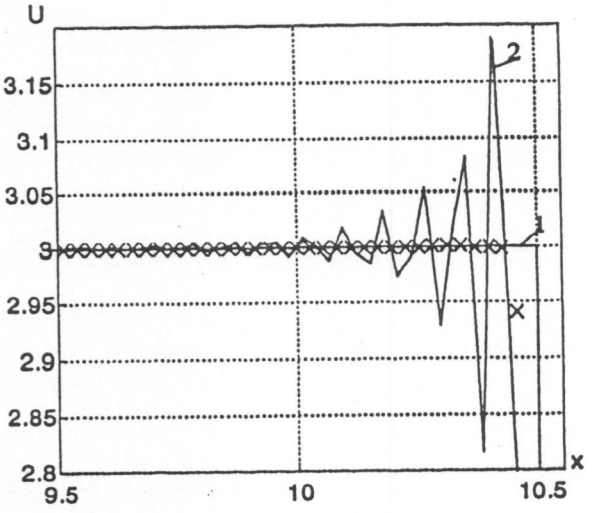

Fig.8. Test ¹1. The dependence of velocity U coordinate x for the shock wave. Fragment of the solution.
1 - analytical solution,
2 - technique [3],
3 - KAMA - 97.

Proposed technique possesses very important asymptotic property. If in a calculation of stationary shock wave the time and grid steps satisfy the condition $\frac{\tau W}{h} = 1$, then in numerical solution shock wave would propagate from one point to another without any dispersion. Profiles of pressure and velocity obtained in calculation of test 1 where time step was chosen under the condition $\frac{\tau W}{h} = 1$ are shown in fig.9,10. Since in this case a+=2.82W the calculation was performed with Courant number $\frac{\tau a_+}{h} = 2.82$. It is seen that under such selection of time step numerical solution precisely coincides with analytical one.

Test 2. Ideal gas with the equation of state

$$P = (\gamma - 1)\,\rho\, E$$

and the following initial parameters:

$$\gamma = 2\ ,\ \rho_0 = 4.5\ ,\ \ E_0 = 1.125\ ,\ P_0 = 5.0625\ ,\ \ U_0 = 0$$

is situated in a region with coordinates [0.,14.]. Constant velocity U = -1 is set at the left boundary of the system.

This problem has the following analytical solution [5]:

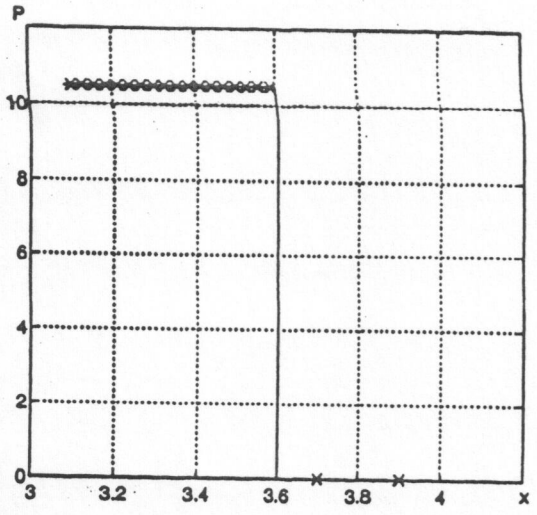

Fig.9. Test [1]. Pressure profile P(x), t=1,029.

$\frac{\tau W}{h}=1$, $\frac{\tau a_+}{h}=2{,}82$

t=1.029.

x x x - calculation,

—— - analytical solution.

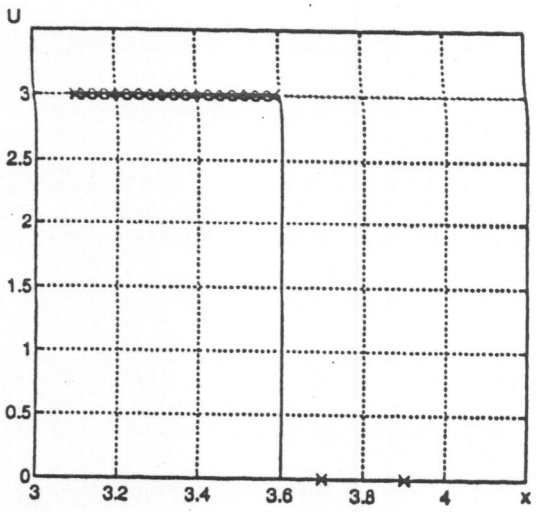

Fig.10.. Test [1]. Velocity profile U(x),t=1.029

$\frac{\tau W}{h}=1$, $\frac{\tau a_+}{h}=2{,}82$

x x x - calculation,

—— - analytical solution

Coordinates of weak discontinuities:

$$x_1 = c_0 t\ ,\ x_2 = \left(c_0 - \frac{\gamma+1}{2}U\right)t\ ;$$

$U(x) = U$, if $x < x_2$,

$U(x) = \frac{2}{\gamma+1}\left(\frac{x}{t} - c_0\right)$, if $x_2 < x < x_1$,

$U(x) = U_0$, if $x > x_1$,

$$\rho = \rho_0\left[1 - \frac{\gamma-1}{2}\frac{|u|}{c_0}\right]^{\frac{2}{\gamma-1}},\quad P = P_0\left[1 - \frac{\gamma-1}{2}\frac{|u|}{c_0}\right]^{\frac{2\gamma}{\gamma-1}}.$$

The profiles of pressure and velocity obtained in numerical solution compared with analytical solution and the calculation using technique proposed in [4] are shown in the figures 11, 12. One can see a good agreement between numerical and analytical solution but there are practically no differences between two calculations if we deal with such scale. Fragments of the solution in the vicinity of weak discontinuity are shown below in the figures 13-20. In these figures the technique "KAMA-97" is compared with techniques from [1], [2], [3,] [4]. It is seen that proposed technique gives smaller oscillations than techniques [1], [3,] [4], and comparing to technique [2] has significantly less "spreading" of weak discontinuity.

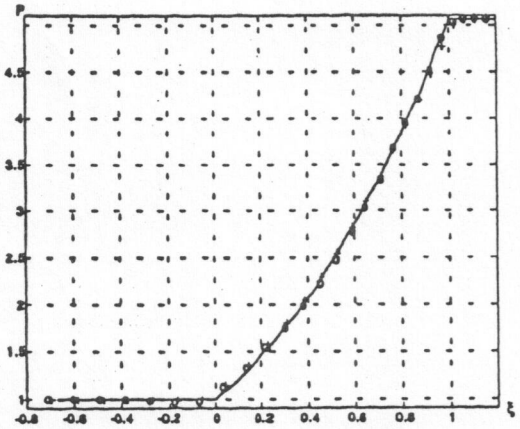

Fig.11. Test ¹2. The dependence of pressure P versus
versus dimensionless coordinate x=x/cΔt for the rarefaction wave, t=2.558
—— - analytical solution,
+ + + - KAMA - 97,
o o o - technique [4].

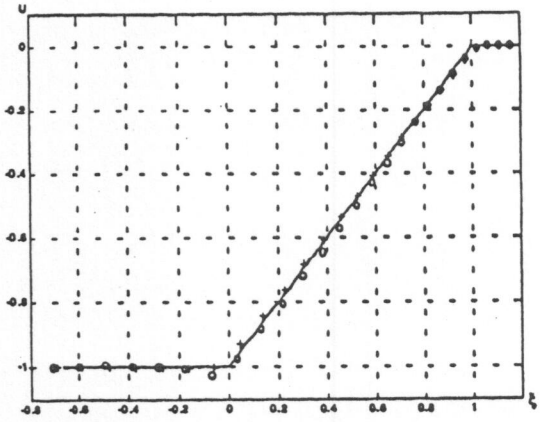

Fig.12. Test ¹2. The dependence of velocity U

dimensionless coordinate x=x/cΔt for the rarefaction wave, t=2.558
—— - analytical solution
+ + + - KAMA - 97,
o o o - technique[1].

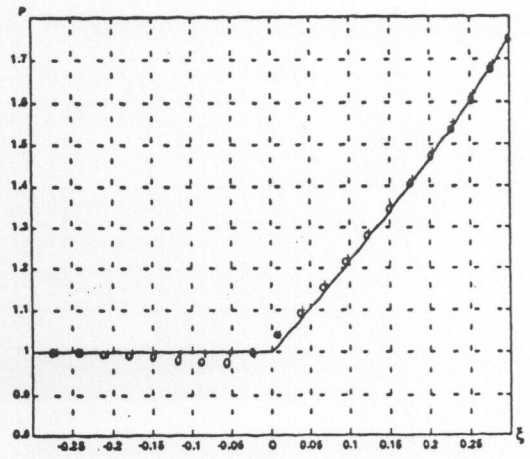

Fig.13. Test ¹2. The dependence of pressure P versus dimensionless coordinate x=x/cΔt for the rarefaction wave, t=4.832

—— - analytical solution,
+ + + - KAMA - 97,
o o o - technique [4].

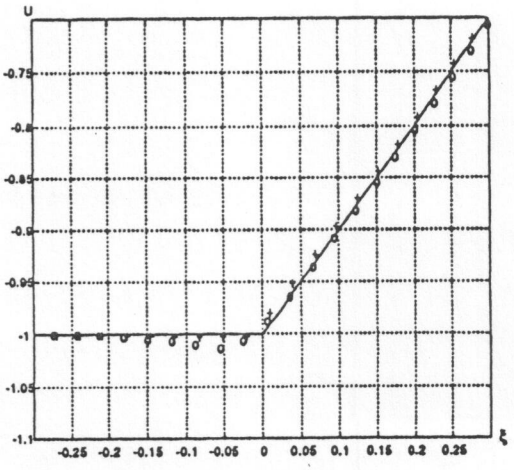

Fig.14. Test ¹2. The dependence of velocity U versus dimensionless coordinate x=x/cΔt for the rarefaction wave, t=4. 832

—— - analytical solution,
+ + + - KAMA - 97,
o o o - technique [4].

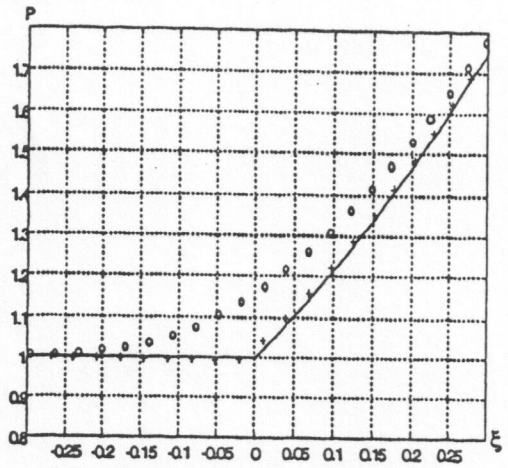

Fig.15. Test ¹2. The dependence of pressure P versus dimensionless coordinate $x=x/c\Delta t$ for the rarefaction wave, t=4. 832
—— - analytical solution,
+ + + - KAMA - 97,
o o o - technique [2].

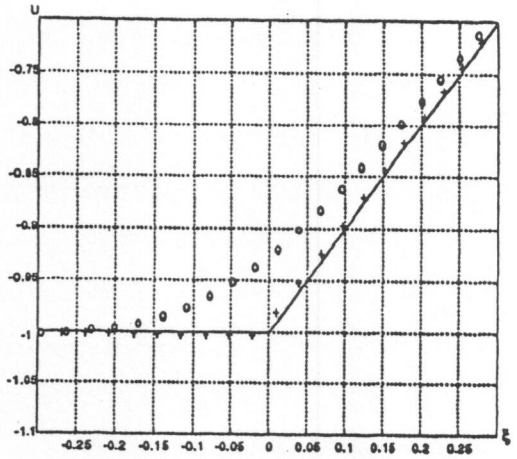

Fig.16. Test ¹2. The dependence of velocity U versus dimensionless coordinate $x=x/c\Delta t$ for the rarefaction wave, t=4. 832
—— - analytical solution
+ + + - KAMA - 97,
î î î - technique [2].

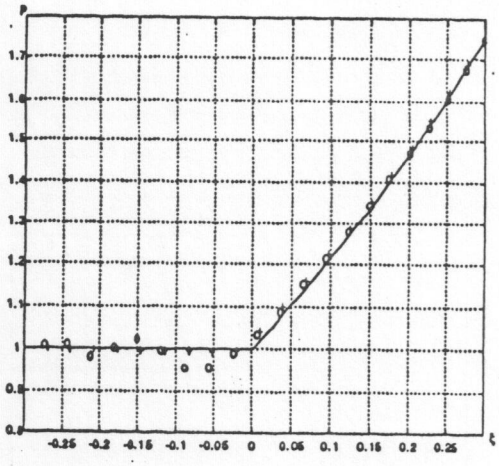

Fig.17. Test ¹2. The dependence of pressure P versus dimensionless coordinate $x=x/c\Delta t$ for the rarefaction wave, t=4. 832
—— - analytical solution,
+ + + - KAMA - 97,
î î î - technique [1].

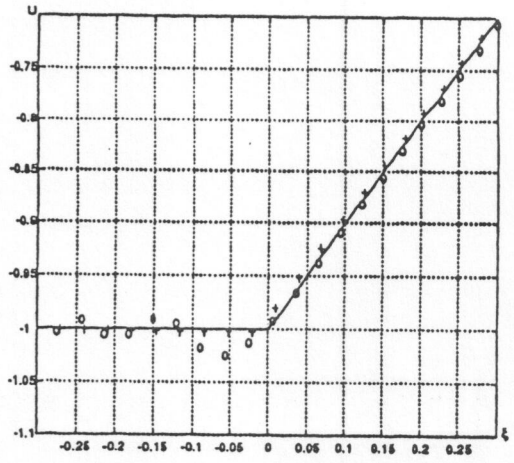

Fig.18. Test ¹2. The dependence of velocity U versus dimensionless coordinate $x=x/c\Delta t$ for the rarefaction wave, t=4. 832
—— - analytical solution,
+ + + - KAMA - 97,
î î î - technique [1].

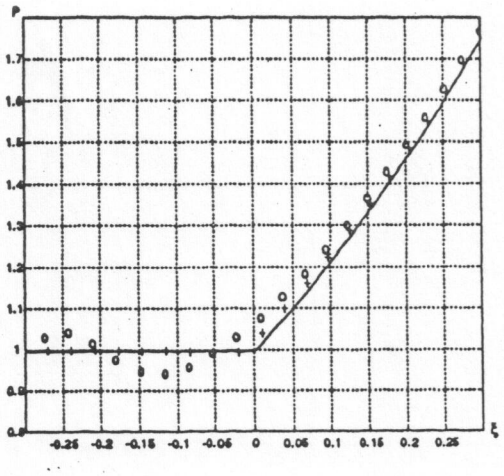

Fig.19. Test ¹2. The dependence of pressure P versus dimensionless coordinate x=x/cΔt for the rarefaction wave, t=4. 832

—— - analytical solution
+ + + - KAMA - 97,
î î î - technique [3]

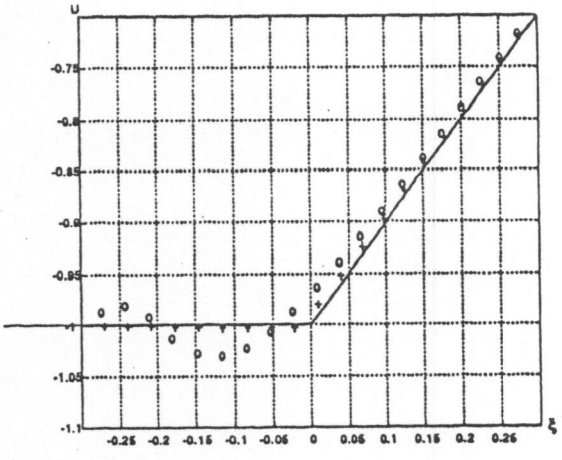

Fig.20. Test ¹2. The dependence of velocity U versus dimensionless coordinate x=x/cΔt for the rarefaction wave, t=4. 832

—— - analytical solution,
+ + + - KAMA - 97
î î î - technique [3].

Tests 3 and 4.

The outcome of shock wave to condensed matter free surface was calculated. Initial data for these problems and flow parameters behind the shock front as well as near the right boundary after shock outcoming are given in table 1.

Table 1
Formulation of tests 3 and 4

	Test 3	Test 4						
Initial data:	r0 Å0	1 0	2,7 0					
U0	0	0						
P0	0	0						
The equation of state P=(g-1)rE + c0k2(r-r0k)			r0k c0k g	1 1 3	2,7	3	3	
Parameters behind the front of the shock wave			U1 P1 r1 f1(S) E1 c1 W	0,75	1,50	1,60	0,342773	
0,28125 1,854049 2,0		1,5 19,65911 3,907477 0,130636 1,125 4,616525 13,106078						
Parameters of the flow near the right boundary in analytical solution when the shock wave comes to right boundary			Urb Ñrb Prb rrb Erb	1,553700 1,050349 0 0,906426 0,051617		3,054503	3,062022	0
2,591729 0,187991								

Constant velocity U = 0.75 was set on the left boundary for the test 3. When the shock wave outcomes to the right boundary discontinuity decay takes place in time Dt=0. In this process the matter should be loaded up to the state behind the shock front according to Hugoniot and then should be released down to pressure P=0 according to isentrope. (P,U)-diagram for this problem is shown in fig.21. When this problem is calculated using homogeneous difference techniques which "spread" strong and weak discontinuities discontinuity decay takes place in time Dt>0. And free surface begins to move when the "head" of "spreaded" shock wave comes to the last calculational mesh. That is why the matter begins to release before it reaches the state behind the shock front. This leads to generation of entropy tracks in the last calculational meshes.

Since Hugoniot relations for strong discontinuities are used for calculating the auxiliary values in the"KAMA-97" technique ,the material in our calculation first is loaded up to the state behind the shock front and then isentropic release takes place (fig.22). That is why entropy tracks are practically absent in the calculations using new technique. The fragment of density profile near the right boundary is shown in fig.23 and the fragment of entropy function is in fig.24. One can see that in calculation using technique "KAMA-97" entropy track is practically absent and in the calculation using technique [4] entropy track is » 50%.

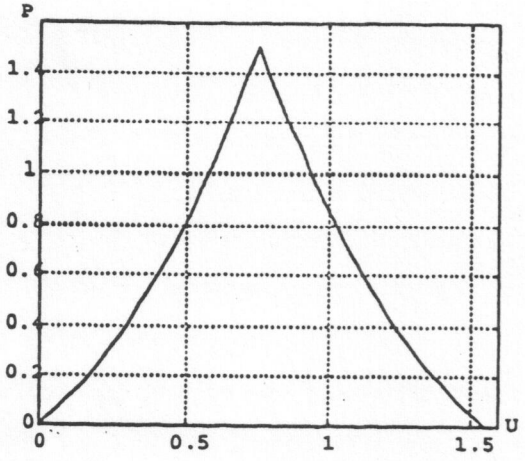

Fig 21. Discontinuity decay when the shock wave comes to a free surface. (P,U)-diagram t=0.7

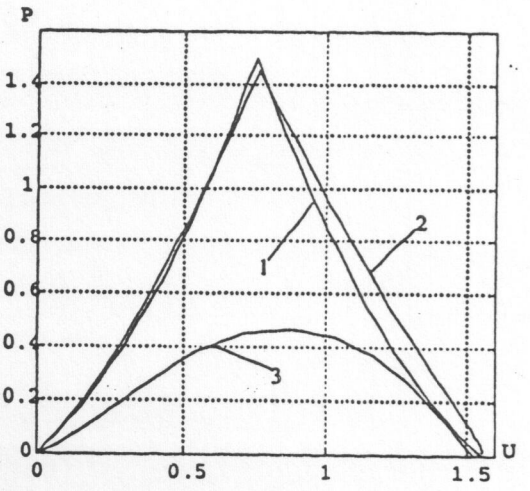

Fig 22. Discontinuity decay when the shock wave function comes to a free surface. (P,U)-diagram.
1 ¾¾ Analytical solution
2 ¾¾ KAMA-97
3 ¾¾ technique [4].

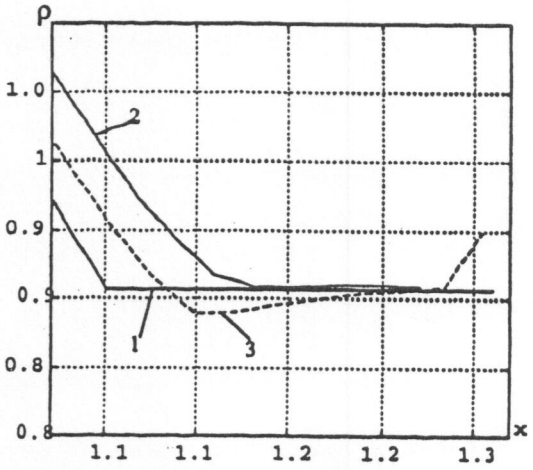

Fig 23. Test 3. The dependence of density r(x),
1 —— analytical solution
2 —— ÊÀÌÀ - 97
3 - - - technique [4].

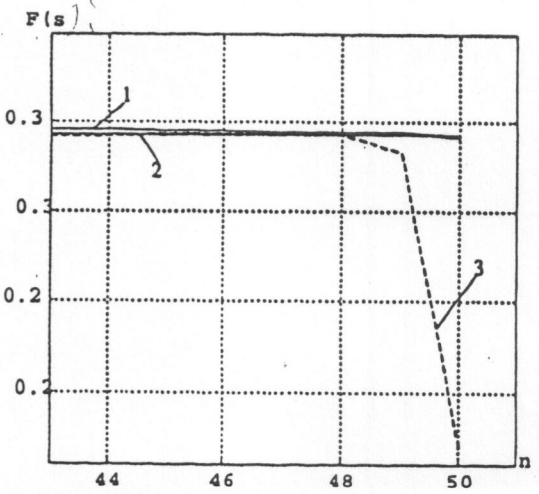

Fig 24. Test 3. The dependence of entropy f(s) versus Lagrangian coordinate
1 —— analytical solution
2 —— ÊÀÌÀ - 97
3 - - - technique [4].(entropy track in f(s) is ~ 50%)

Variable boundary condition U(t) ensuring construction of analytical solution was set on the left boundary. The form of dependence U(t) is shown in fig.25.

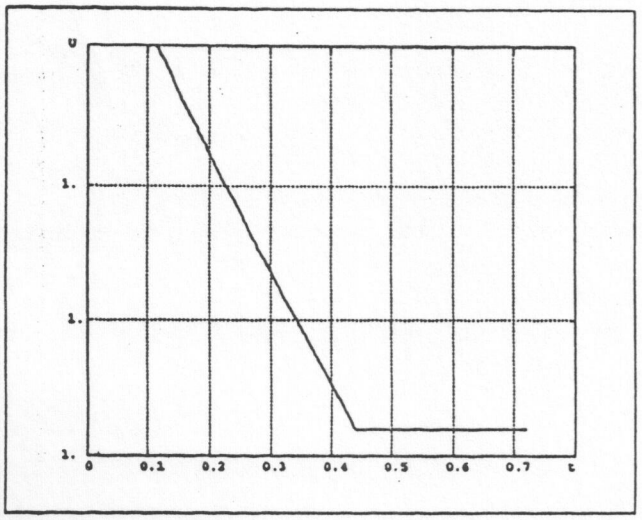

Fig.25. Test 4. The form of boundary condition U(t)

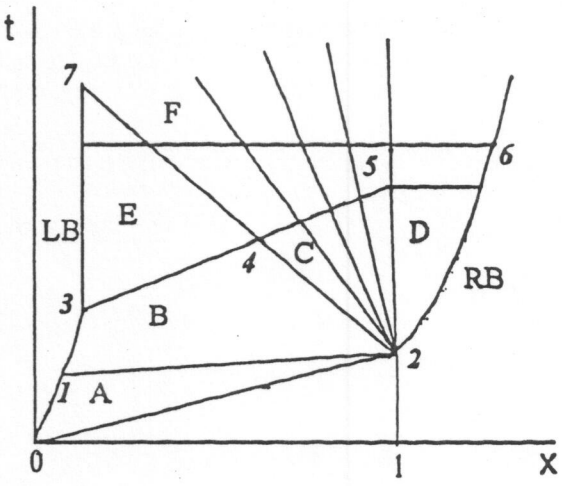

Fig 26 X-t diagram

(X,t)-diagram for analytical solution of problem 4 is shown in fig.26. Stationary shock wave is in zone A, rarefaction wave propagating from left boundary is in zone B, interaction of two rarefaction waves takes place in zone C, in zone D flow parameters are determined by the rarefaction wave propagating from left boundary and by zero pressure on the right boundary. Here pressure minimum at each time t >t1 is achieved on the characteristic (2-5). At time t5 pressure achieves the value when material fails. Boundary condition Ulb(t) was set in such a manner that failure takes place only in one point. Calculational dependence of minimum pressure Pmin versus a number of calculational mesh (mass Lagrangian coordinate) is shown in fig.27. Material failure takes place when Pmin= -1. Calculation is in good agreement with analytical solution.

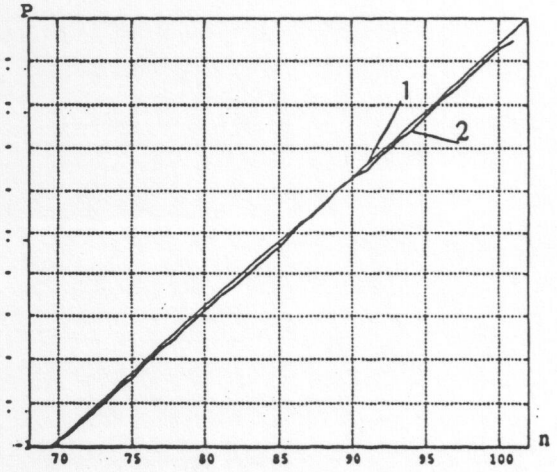

Fig.28. Test 4. Dependence of Pmin versus the number of calculational mesh (versus mass). Matter destruction takes place when Pmin = -1.

1 - analytical solution

2 - calculation KAMA-97

Thus due to specific form of difference equations and application of Hugoniot-Renkin relations for description of energy dissipation inside of shock layer oscillation and dispersing properties of difference technique were minimized, we succeed in elimination of entropy tracks when shock wave outcomes to free surface and accuracy in calculation of spoll mass was elevated.

REFERENCES

1. J.Neumann, R.Richtmayer. A method for the Numerical Calculation of Hydrodynamical Shocks. - J. Appl.Phys. - 1950. - 21, ¹3 . - p. 232-237.
2. S.K.Godunov. Difference Technique for Calculations of Discontinuous Solutions for Gas Dynamic Equations. - Mathematical collection. - 1959. - v.47(89), issue 3. - p.271-306.
3. P.Lax, B.Wendroff. System of Conservation Laws. -Comm. Pure Appl. Math. - 13 - 1960 - 217
4. V.F.Kuropatenko. On Difference Techniques for Hydrodynamic Equations. - Transactions of Mathematical Institute namrd after V.A.Steklov. - v.74. - Moscow. - 1966. - p.107-137.
5. R.Richtmayer, K.Morton. Difference Techniques for Solution of Boundary-value Problems. - Moscow - "Mir" -1972